Journal of Materials Science & Technology 65 (2021) 29–37

Contents lists available at ScienceDirect

Journal of Materials Science & Technology

journal homepage: www.jmst.org

Research Article

Strengthening and ductilization of laminate dual-phase steels with high martensite content

Bo Gao[a,1], Rong Hu[b,1], Zhiyi Pan[a], Xuefei Chen[c,d], Yi Liu[a], Lirong Xiao[a], Yang Cao[a], Yusheng Li[a], Qingquan Lai[b,*], Hao Zhou[a,*]

[a] Nano and Heterogeneous Materials Center, School of Materials Science and Engineering, Nanjing University of Science and Technology, Nanjing 210094, China
[b] Herbert Gleiter Institute of Nanoscience, Nanjing University of Science and Technology, Nanjing 210094, China
[c] State Key Laboratory of Nonlinear Mechanics, Institute of Mechanics, Chinese Academy of Sciences, Beijing 100190, China
[d] School of Engineering Science, University of Chinese Academy of Sciences, Beijing 100049, China

ARTICLE INFO

Article history:
Received 20 January 2020
Received in revised form 15 March 2020
Accepted 19 March 2020
Available online 12 July 2020

Keywords:
Dual phase steel
Warm rolling
Laminate structure
Bauschinger effect
HDI stress

ABSTRACT

The steels with excellent strength and ductility are expected to be achieved by tailoring the microstructural features. In this work, laminate dual-phase (DP) steels with high martensite content (laminate HMDP steels) were produced by a combination of warm rolling and intercritical annealing. Influence of rolling strain and annealing temperature on the microstructural evolution and mechanical properties of laminate HMDP steels were systematically studied. The strength of HMDP steels was significantly improved to ~1.6 GPa associated with a high uniform elongation of 7%, as long as the laminate structure is maintained. The strengthening and ductilizing mechanisms of laminate HMDP steels are discussed based on the influence of laminate structure and the high martensite content, which promote the development of internal stresses and can be correlated to the Bauschinger effect as measured by the cyclic loading-unloading-reloading experiments. Detailed transmission electron microscopy (TEM) observation was applied to characterize the dislocation structure in the deformed ferrite.

1. Introduction

Ferrite-martensite dual-phase steels have been widely used in various applications due to the advantages of low cost, easy to process and reasonable mechanical performance [1,2]. But the improvement of mechanical properties of DP steels is continuously pursued in order to fulfill the increasingly stringent design requirements. Numerous strategies are developed to achieve a good combination of strength and ductility of DP steels, including sophisticated alloy design and thermomechanical processing routes, which turns out to be engineering the heterogeneities at various scales [3–6].

Structural refinement is an efficient method to strengthen the metallic materials [7]. In recent decades, novel techniques of severe plastic deformation (SPD) are developed to refine the grain size of metallic materials to ultra-fine and even nano scale [8–10]. Ultra-fine grained/nanocrystalline (UFG/NS) materials usually show extraordinarily high strength, at the expense of ductility owing to the limited strain hardening capacity [11,12]. For example, the nanostructured plain low-carbon steel with a high strength of 1.2 GPa was produced by using dynamic plastic deformation while it presents no useful ductility [13]. The concept of heterostructured materials (HSMs) is proposed to enhance the strain hardening capacity of the UFG/NS materials [14,15]. These materials have a dramatic difference in strength between different zones, while the sizes of the zones could be in the range of micrometers to millimeters. Due to the significant strength mismatch between different zones in HSMs, inhomogeneous deformation occurs in the local areas as well as the elasto-plastic incompatibility. During the deformation of heterogeneous structural materials, a set of internal stresses are developed by the stress partitioning to the stronger zones and/or by the generation of GNDs in the softer zones adjacent to the interface, resulting in an enhanced strain hardening [16,17]. Recently, it is found that exploring the heterogeneity to the limit of a strong matrix surrounding the soft region, which involves a laminate morphology, presents a superior combination of strength and ductility [14].

* Corresponding authors.
E-mail addresses: lai@njust.edu.cn (Q. Lai), hzhou511@njust.edu.cn (H. Zhou).
[1] The authors contributed equally to this work.

https://doi.org/10.1016/j.jmst.2020.03.083
1005-0302/

The engineering of DP steels could be inspired by the abovementioned HSMs approach. The mechanical property of martensite phase is analogous to nanocrystalline zones in HSMs, in terms of the high strength and limited ductility while the ferrite shows low strength and high ductility, which is almost same to the properties of coarse-grained zones in HSMs [18,19]. Therefore, steels composed of dominant martensite matrix and minor ferrite phase could be expected to present excellent strength and ductility, which is called HMDP steels, in contrast with the conventional DP steels with 20–30 vol % martensite phase [20–22]. However, the efficiency of HMDP is yet to be examined as well as the strengthening and ductilizing mechanisms.

This study is dedicated to producing the laminate HMDP microstructures and to investigating the deformation behavior in details. Warm rolling and subsequent controlled intercritical annealing were carried out to produce the laminate HMDP steels. The microstructure generation and mechanical properties of the laminate HMDP steels were systematically investigated. In addition, according to the cyclic load-unload-reload (LUR) tensile tests and the detailed TEM observations of dislocation substructures, the in-depth physical mechanisms of strengthening and ductilization of laminate HMDP steels were discussed.

2. Materials and methods

The chemical composition of the studied low-carbon steel was Fe-0.2C-1.37Si-1.94 Mn in weight percent, which was determined by a vacuum emission spectroscopy. Hot-rolled plates with thickness of 3.8 mm were used as the starting material. As shown in Fig. 1(a), the as-received microstructure was composed of layers of ferrite and pearlite, which have average thicknesses of 4.1 μm and 2.9 μm, respectively. As illustrated in Fig. 1(b), the as-received steel plates were warm rolled at 600 °C to a total reduction of 40 % and 60 %, respectively. The rolled plates were then intercritically annealed (at 780, 800 and 840 °C) for 2 min and water quenched to room temperature. Warm rolling was applied due to its advantages in processing. Firstly, the initial ferrite + pearlite microstructure gets hardened rapidly by the rolling deformation, but warm rolling involves a lower rolling resistance than cold rolling [23]. Secondly, the warm rolling process can accelerate the cementite spheroidization, which provides more nucleation sites for the austenite formation during intercritically annealing to form fine-grained DP steel [24,25]. The rolling temperature of 600 °C was thus set to facilitate the abovementioned advantages, while minimizing the recrystallization of ferrite during processing.

Dog-bone-shaped tensile specimens with a gauge length of 10 mm and a width of 2.5 mm were cut from the plates with the longitudinal axes parallel to the rolling direction. The tensile specimens were polished to a mirror finish before tensile test. Quasi-static uniaxial tensile tests were performed in a LTM-20KN testing machine with a strain rate of 3×10^{-3} s^{-1} at room temperature. The cyclic LUR tensile tests were performed to measure the Bauschinger effect following the procedure in previous studies [17,26]. During the LUR tensile tests, the specimens were tensioned to an assigned strain, unloaded to 50 N, and then reloaded.

The cross-section samples were grinded and polished and etched with the 5% Nital solution. The microstructures were observed by a scanning electron microscopy (SEM, FEI Quanta 250 F). The volume fraction of martensite was measured using the Image J software, following the procedure in Ref. [27]. TEM observations were performed on a FEI TECNAI 20 electron microscopy operated at 200 kV. The TEM specimens were cut parallel to the normal plane and grinded to a thickness of ~60 μm. Perforation by twin-jet polishing machine was carried out using a solution of 20 % perchloric acid and 80 % methanol at −35 °C.

3. Results and discussion

3.1. Microstructures

As shown in Fig. 2, warm rolling results in a laminate morphology. The average thicknesses of the ferrite layers are reduced to 3.2 and 1.7 μm with rolling reductions of 40 % and 60 %, respectively. Spheroidized cementite particles with size less than 80 nm are uniformly distributed in the prior pearlite zones, as shown in Fig. 2(a-2) and (b-2). A larger warm rolling reduction results in a higher degree of spheroidization. This observation is consistent with the reported accelerated spheroidization in warm deformed pearlitic steels [28,29]. In addition, the cementite particles are also found along the ferrite grain boundaries. The intergranular cementite particles are suggested as obstacles to impede ferrite recrystallization and grain growth during deformation and heat treatment at high temperatures [30].

Fig. 3(a-1)-(a-3) shows that the volume fraction of martensite increases with increasing annealing temperature in the 40 % warm rolled samples. The laminate structures are generally maintained after intercritical annealing due to the short annealing time, especially in the samples annealed at 780 °C and 800 °C. Most of the martensite zones are at the locations of prior pearlite, with only limited martensite islands inside the ferritic grains. The sample annealed at 840 °C has the highest volume fraction of martensite and the minor ferrite is fully isolated by the surrounding martensitic matrix. Fig. 3(b-1)-(b-3) shows the microstructure of the intercritically annealed samples involving a rolling reduction of 60 %. The thickness of laminate ferrite is smaller than that of 40 % rolling reduction. However, the laminate structure is almost destroyed in the sample annealed at 840 °C and the microstructure is more closed to a martensitic structure, as shown in Fig. 3(b-3).

The volume fraction of martensite is significantly affected by both the annealing temperature and rolling reduction. Fig. 4 shows that when the annealing temperature is increased from 780 °C to 800 °C and 840 °C, the volume fraction of martensite of the 40 % warm-rolled sample is increased from 50 % to 57 % and 70 %, respectively. However, the martensite fraction is increased from 60 % to 67 % and 88 % in the 60 % warm-rolled samples annealed at 780 °C, 800 °C and 840 °C, respectively. With higher rolling reduction, the simultaneous ferrite grain refinement and accelerated cementite spheroidization result in a larger number of carbide particles at the ferrite grain boundaries, which are the preferred austenite nucleation sites, and the kinetics of austenite formation is thus enhanced [24,31]. Notice that the difference in martensite content for the DP steels annealed at the same temperature should be diminished when the annealing time is sufficiently long as to reach thermodynamic equilibrium. But previous short soaking time of 2 min is not enough for the process of austenitization to be completed in the studied steels [32,33].

Fig. 5 schematically illustrates the microstructure evolution of warm-rolled DP steel during intercritical annealing. The warm-rolled DP steel has a laminate structure of ferrite and pearlite, but the cementite has been spheroidized. A larger rolling reduction results in a higher degree of spheroidization, introducing more spheroidized carbides locating at ferrite grain boundaries. During intercritical annealing, the carbides tend to dissolve and trigger austenite formation. But numerous investigations have shown that only the carbide particles at the ferrite grain boundaries provide the most potent austenite nucleation sites, due to the interface triple junction and the fast diffusion along grain boundaries [34–36]. Therefore, with higher degree of warm rolling, the ferrite grains are finer with a higher fraction of spheroidized carbides, thus providing more austenite nucleation sites to promote austenite formation.

TEM observations were carried out to investigate the 40 % warm-rolled laminate HMDP microstructures after annealing at different

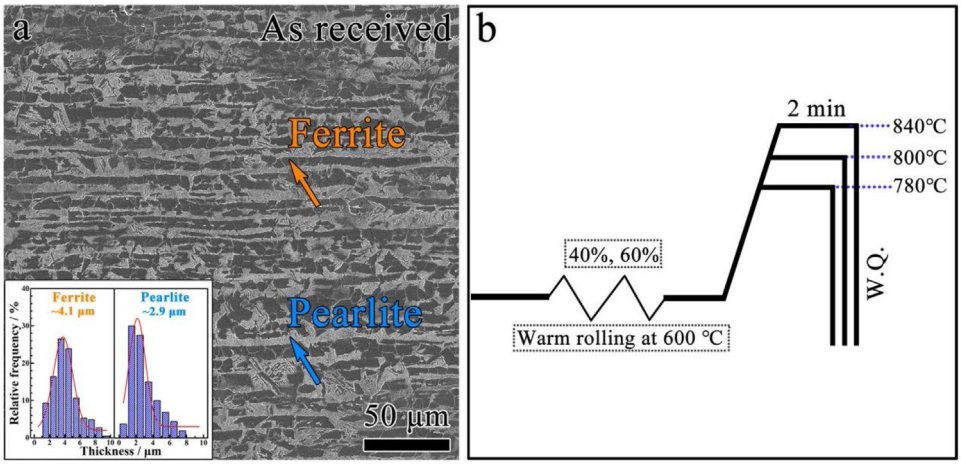

Fig. 1. (a) SEM image of as-received DP steel and (b) schematic diagram of the processing routes.

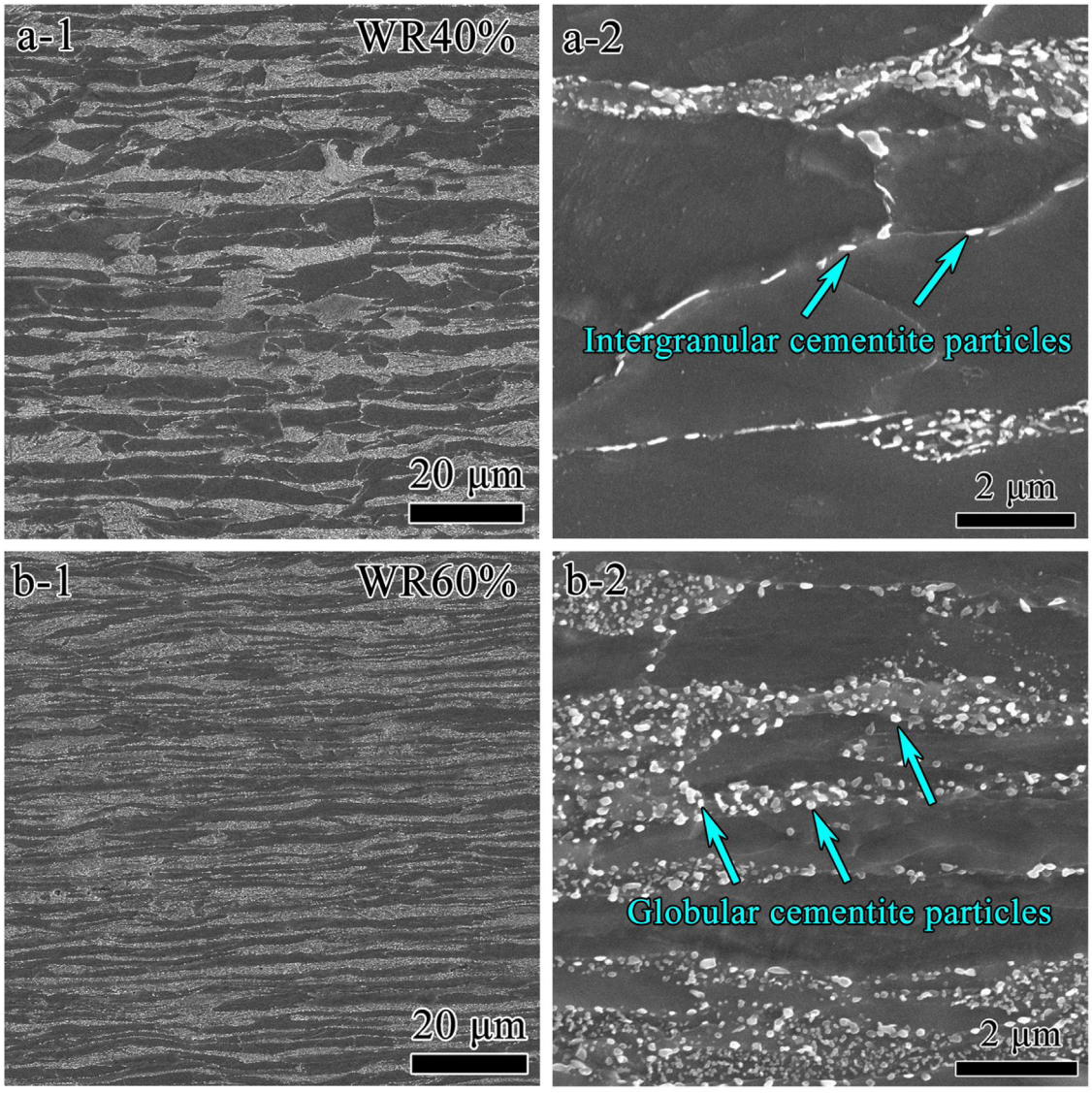

Fig. 2. SEM images of the low carbon steels rolled at 600 °C: (a-1, a-2) with 40 % thickness reduction; (b-1, b-2) with 60 % of thickness reduction.

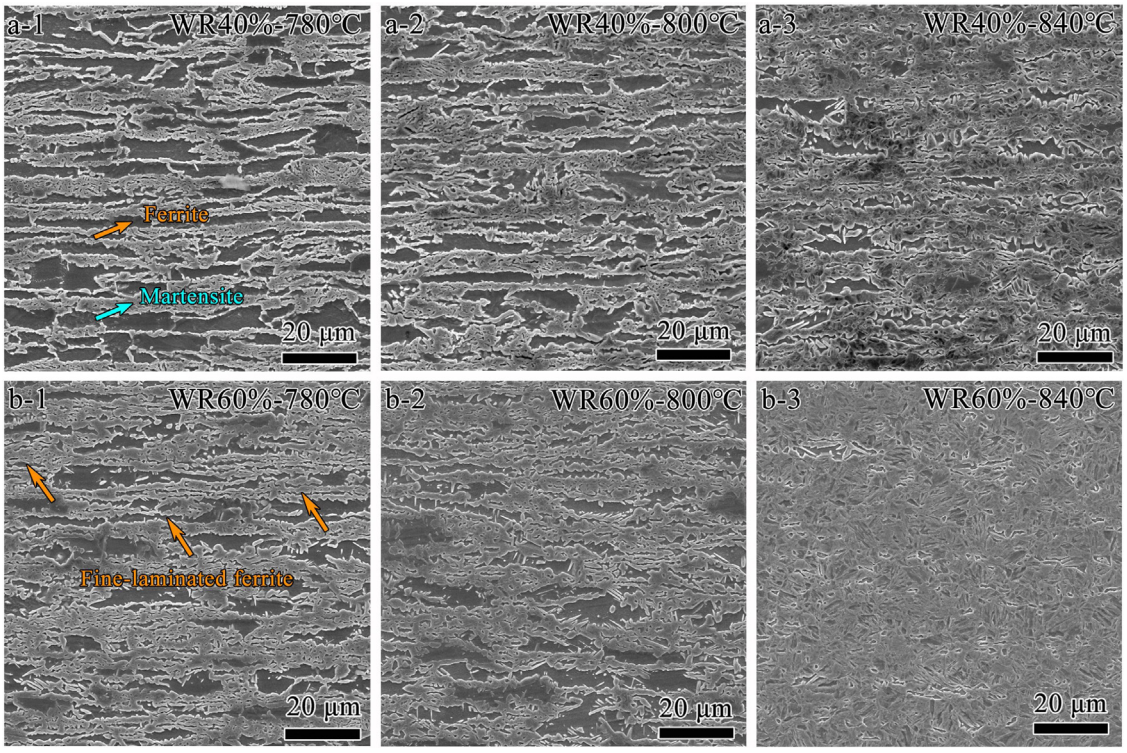

Fig. 3. SEM images of intercritical annealed DP steels: (a-1, a-2, a-3) the 40 % warm-rolled samples annealed at 780 °C, 800 °C and 840 °C, respectively; (b-1, b-2, b-3) the 60 % warm-rolled samples annealed at 780 °C, 800 °C and 840 °C, respectively.

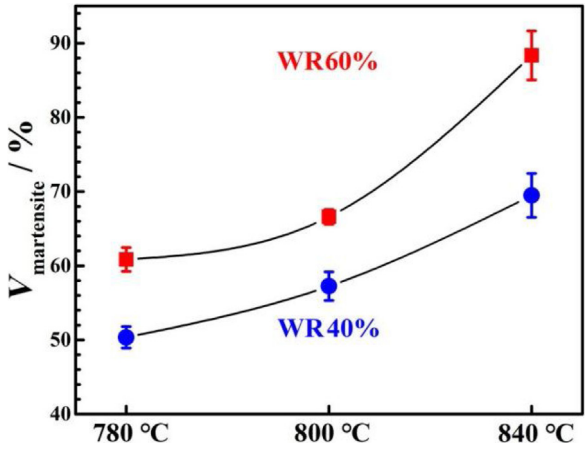

Fig. 4. Volume fraction of martensite of the warm-rolled (WR) steels after annealing at different temperatures.

temperatures. Fig. 6(a) shows that the small martensite islands in size of ~200 nm are distributing along the ferrite grain boundaries. High density of dislocations are concentrated in the ferrite adjacent to the ferrite/martensite interface, probably due to the local deformation to accommodate the martensitic transformation [37]. The dislocations at the interface region are tangled, while those in the grain interior are more isolated and straight. As the annealing temperature increased to 800 °C, significant growth of martensite is observed surrounding the ferrite grains, as shown in Fig. 6(b). As a result, the grain size of ferrite reduces to ~3 μm, which achieves grain refinement by a thermal processing method without plastic deformation. The benefits of phase transformation in grain refinement has also been explored in a recent study, in which Tsuji et al. proposed a novel thermomechanical processing to produce UFGs in low-carbon steel without SPD [38]. Fig. 6(c) shows that the grain size of ferrite is refined to ~1 μm after annealing at 840 °C. The ultra-fine ferrite grains are embedded in the martensite domains, which is the proposed heterostructure to enhance the strength and ductility of materials [15].

3.2. Mechanical properties and strengthening mechanism

Fig. 7(a) and (b) shows the tensile stress-strain curves of the laminate HMDP steels. The strength and elongation are listed in Table 1. As the annealing temperature is increased from 780 °C to 800 °C and 840 °C, the yield strength (YS) of 40 % warm-rolled sample is increased from 677 MPa to 776 MPa and 1109 MPa, and the ultimate tensile strength (UTS) is increased from 1183 MPa to 1342 MPa and 1559 MPa, respectively. While in the 60 % warm-rolled samples, the YS of 60 % warm-rolled sample is increased from 831 MPa to 1017 MPa and 1349 MPa, and the UTS is increased form 1361 MPa to 1485 MPa and 1648 MPa, respectively. Higher martensite

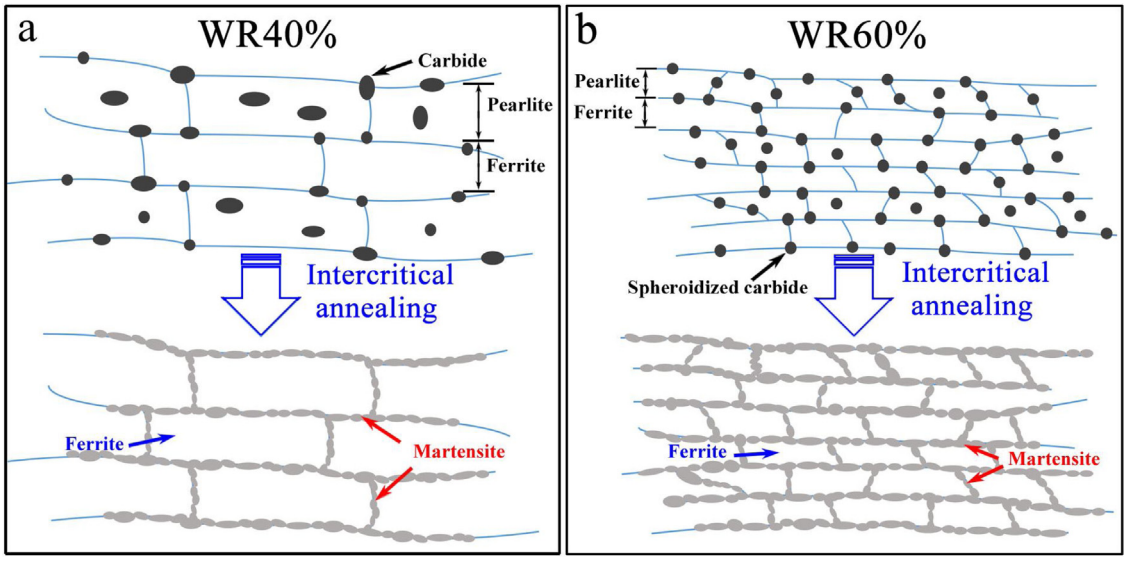

Fig. 5. Schematic illustration of microstructural evolution of intercritically annealing: (a) WR40 %; (b) WR60 %.

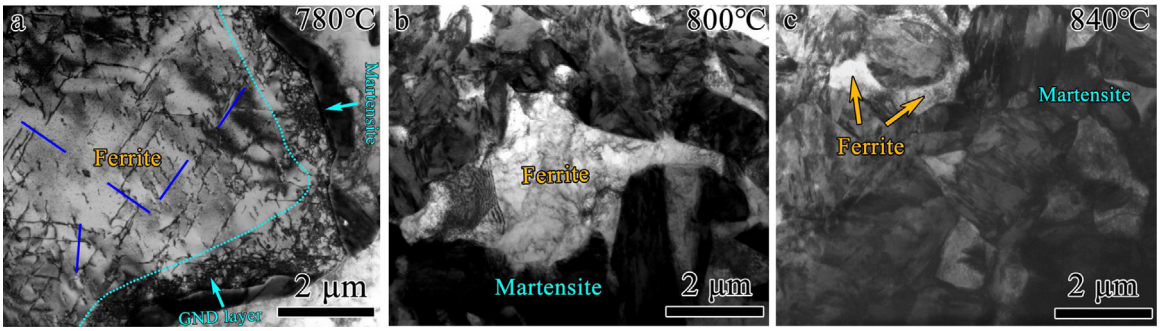

Fig. 6. TEM images of the 40 % warm-rolled DP steels annealed at (a) 780 °C, (b) 800 °C and (c) 840 °C.

Table 1
Tensile properties of the warm rolled DP steels annealed at 780 °C, 800 °C and 840 °C.

Thickness reduction	Temperature (°C)	YS (MPa)	UTS (MPa)	UE (%)
40 %	780	677	1183	8.6
	800	776	1342	8.0
	840	1109	1559	7.1
60 %	780	831	1361	8.4
	800	1017	1485	6.9
	840	1349	1648	4.6

fraction increases both the YS and UTS of DP steels, but also leads to a reduction of uniform elongation (Fig. 7(c)) [39–41]. The reduction of UE in 60 % warm-rolled samples (from 8.4 % to 4.6 %) is much larger than that of 40 % warm rolled samples (from 8.6 %–7.1 %), as listed in Table 1. The 40 % warm-rolled samples derive their high ductility from their high strain-hardening rate (Θ=dσ/de; σ: stress, e: strain), as shown in Fig. 7(d). The 40 % warm-rolled samples have higher strain hardening rate than the 60 % warm-rolled samples during tensile test. Compared with the samples annealed at 780 °C and 840 °C, especially in the 60 % warm-rolled samples, the Θ shows a steep drop at first. However, as the tensile strain is increased to 4 %, the slope of strain hardening curves of sample annealed at 780 °C shows significant decrease, which retards the onset of necking to a larger strain of 8.4 %.

The outstanding strain hardening of DP steels is usually attributed to its composite nature. The heterogeneities of the DP steels could result either in the non-uniform deformation, the associated strain gradient enhancing the generation of GNDs, or in the stress partitioning among domains of different mechanical strength during deformation. These mechanisms involve the development of internal stresses at different scales, which contribute to the strain hardening. This contribution is recently termed as hetero-deformation-induced (HDI) stress in Ref. [17] and can be evaluated by the Bauschinger-type cyclic LUR tensile tests, as shown in the hysteresis in Fig. 8(a). The HDI stress is calculated by the following equations [17,26]:

$$\sigma_{HDI} = \sigma_{flow} - \sigma_{eff} \quad (1)$$

$$\sigma_{eff} = \frac{\sigma_{flow} - \sigma_u}{2} + \frac{\sigma^*}{2} \quad (2)$$

where σ_{flow} is the flow stress, σ_{eff} is the effective stress, σ_u is the reverse yield stress and σ^* is the thermal part of the flow stress related to viscous flow at the initiation of unloading, as schematically shown in Fig. 8(b).

As shown in Fig. 8(c), HDI stress is increased with the applied strain, and the magnitude of HDI stress is increased with the martensite content. Fig. 8(d) presents the hysteresis loops obtained from the LUR tensile tests, following the procedure in Ref. [42], which is an alternative method of evaluating the magnitude of Bauschinger effect. The area of the loops increases with strain and the DP steels with higher martensite content generally present a larger hysteresis, indicating a stronger Bauschinger effect, which is consistent with the assessment by the HDI stress as shown in Fig. 8(c). However, for the 60 % warm-rolled sample annealed at

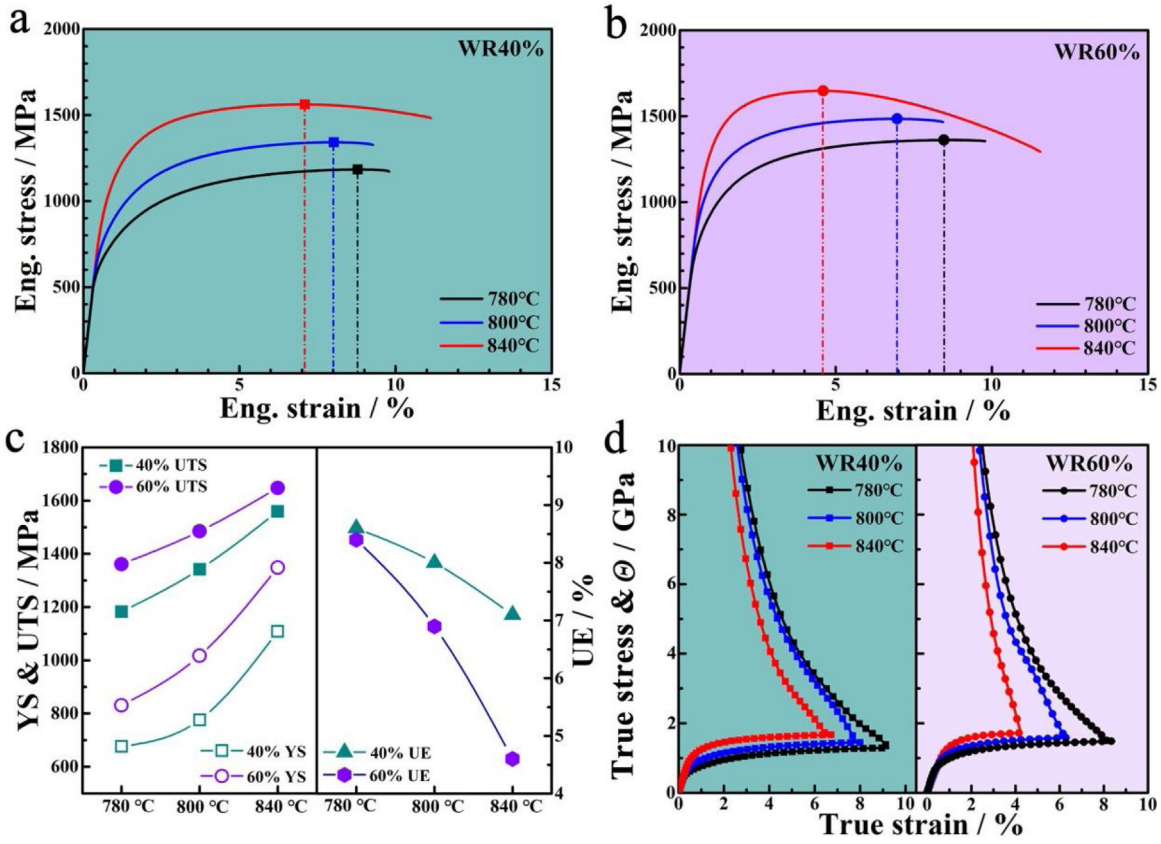

Fig. 7. Effect of rolling strain and annealing temperature on the mechanical behaviors of DP steels. Engineering stress-strain curves of the samples with (a) 40 % rolling reduction and (b) 60 % rolling reduction. (c) Evolution of YS, UTS and UE at different annealing temperatures and (d) strain hardening rate curves from tensile tests.

840 °C, the Bauschinger effect is reduced to the lowest level, which is related to the deformation highly dominated by the martensite phase and the microstructure should be considered essentially as martensitic.

The good combination of strength and ductility, as well as the remarkable Bauschinger effect is attributed to the microstructural features of the laminate HMDP steel. First, enhanced strength level of the laminate HMDP steels is related to the higher volume fraction of martensite and the associated mechanical constraint to ferrite. This phenomenon has been explored by the finite element modeling works [43,44] that the local stress in ferrite is higher in a DP microstructure with larger amount of martensite. This constraint effect is contributied to the high strength achieved in the studied microstructures, which is also anticipated in the proposed heterostructured materials concept [14,15].

Second, larger volume fraction of martensite results in a lower local carbon content, which improves the formability and the strain carrying capacity of the martensite phase. The meso-scale strain distribution should be more uniform when the martensite volume fraction is further increased. The situation is approaching to the situation of iso-strain condition. Therefore, the load transfer efficiency is higher, promoting the development of internal stresses distribution between the strong martensite and soft ferrite, which has been clearly revealed by the experimental and numerical investigations in [1,45]. The sufficient ductility of martensite is a pre-requisite, which is allowed for by the lower carbon content partitioned to the prior austenite region during intercritical annealing, preventing premature failure due to the early fracture of martensite phase [46,47]. In that sense, the essential heterogeneity in this case is not about the non-uniformity of strain as in the conventional DP steels, but is referred to the mechanical heterogeneity between constituent phases, which results in the elasto-plastic incompatibility during deformation. Therefore, the higher magnitude of HDI stress with increasing martensite volume fraction is due to the stress partitioning, by which the ferrite is under higher compression stress and gets yielded earlier during unloading. The resulting HDI stress increases the overall flow stress through a kinematic hardening contribution, which enhances strength and propones the onset of necking.

3.3. *Dislocation substructure evolution during tensile testing*

In conventional DP steels, the non-uniform deformation results in the plastic strain primarily concentrated in ferrite, and the associated strain gradient enhances the generation of GNDs [48,49]. But as mentioned above, the laminate DP steels with increasing martensite volume fraction is imposing a more uniform meso-scale deformation, which must impact the formation of dislocation substructures. Representative TEM observations on the 60 % warm-rolled sample annealed at 780 °C and the 40 % warm-rolled sample annealed 840 °C (termed as 60 %–780 DP and 40 %–840 DP), which were interrupted at a tensile strain of 6%, were conducted to examine the development of the dislocation substructures in ferrite of the laminate HMDP steels. These two microstructures involve the martensite volume fractions of 60 % and 70 %, respectively. Fig. 9(a-1) shows the dislocation substructure in the ferrite zone adjacent to martensite in the 60 %–780 DP steel after pre-tension. Generally speaking, the dislocations are uniformly distributing within the ferrite phase, including the grain interior and the region close to the interfaces. Dislocation tangles and dislocation walls are clearly shown in Fig. 9(a-2). This is different with the as-quenched state as shown in Fig. 6, in which a layer of GNDs at the interface are generated due to the martensitic transformation. As to the 40 %–840 DP steel with a higher martensite volume fraction, a high den-

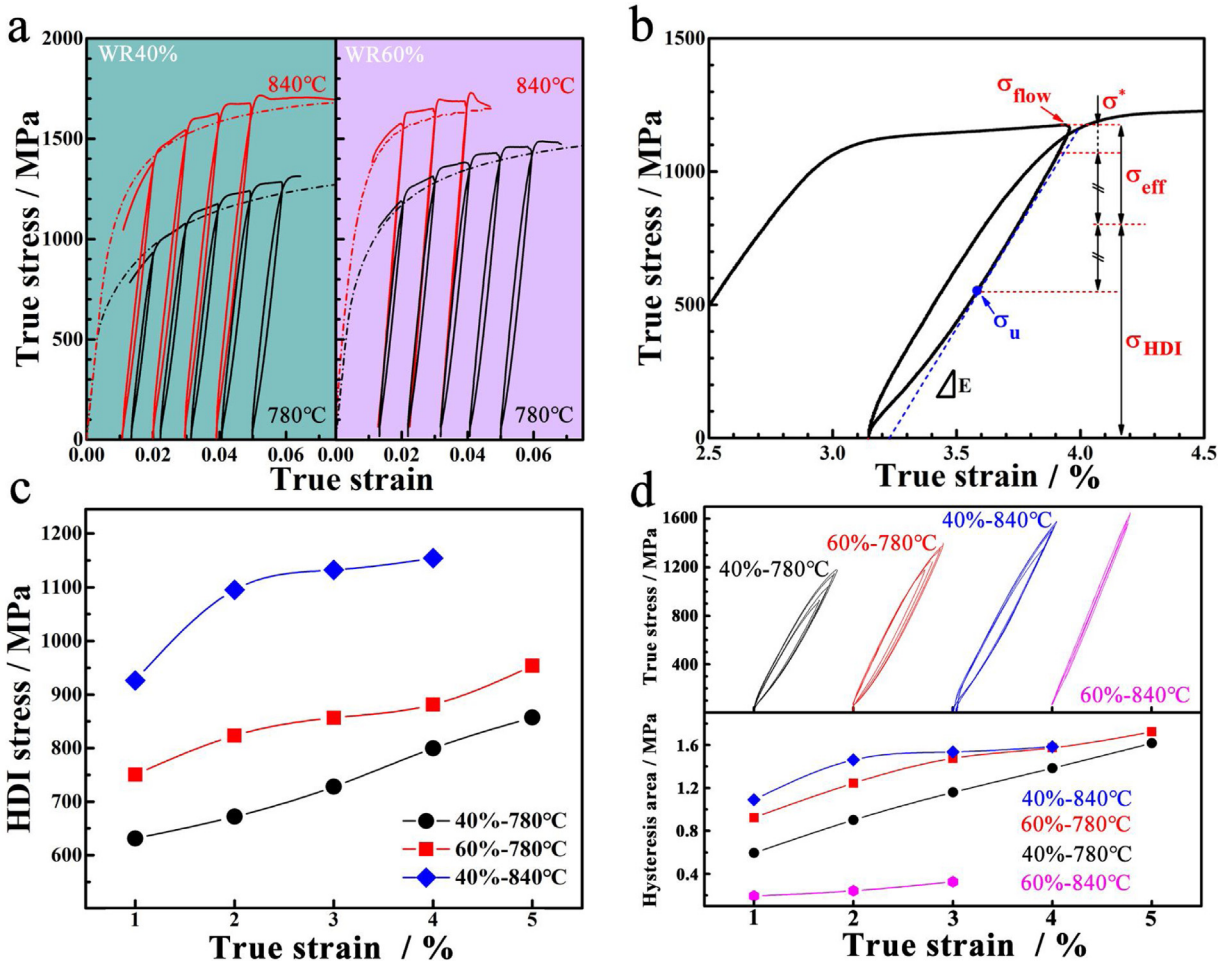

Fig. 8. LUR tensile tests: (a) the load-unload-reload curves of dual phase steels. (b) Schematic of hysteresis loops for characterizing the Bauschinger effect. (c) Evolution of HDI stress with applied strain. (d) Load-unload curves (hysteresis loops) and the hysteresis areas of HMDP steels varying with true strain. The loops have been shifted in strain for comparison.

sity of dislocations is accumulated throughout the ferrite grain that is imbedded in the martensite, with a rather uniform distribution, as shown in Fig. 9(b-1) and (b-2). Although the present bright-field TEM micrographs cannot examine the nature of dislocations, SSDs or GNDs, a uniform distribution of dislocations within the ferrite phase is consistently revealed. According to Refs. [50,51], the GNDs can be considered as additional contribution to forest hardening as similar as SSDs, and the observed dislocation substructures suggest a rather homogeneous glide resistance of dislocations within ferrite. This is also consistent with the interpretation of the deformation mechanism of the laminate HMDP steels, in which the meso-scale deformation is more uniform with a high martensite volume fraction and the development of meso-scale internal stresses is the major contribution to the strengthening and ductilization.

4. Conclusions

Low-carbon laminate HMDP steels were prepared via warm rolling at 600 °C, followed by intercritical annealing and quenching. Warm rolling was applied due to its advantages in processing, including the lower rolling resistance and accelerated cementite spheroidization that provides more austenite nucleation sites and enhances the kinetics of austenite formation. Influence of rolling strain and annealing temperature on microstructural evolution and mechanical properties were systematically studied. The in-depth mechanism of strengthening and ductilization of the laminate HMDP steels were discussed. The key findings are summarized as follows:

(1) Laminate ferrite + pearlite low-carbon steels were produced by warm rolling at 600 °C. With rolling reduction of 40 % and 60 %, the laminate thickness was effectively refined to average sizes of ~3.2 μm and ~1.7 μm, respectively.
(2) The laminate HMDP steels with volume fraction of martensite above 50 % were produced by intercritical annealing of the warm rolled samples. The laminate structures are maintained after intercritical annealing due to the short annealing time, especially in the samples annealed at 780 °C and 800 °C. The volume fraction of martensite was significantly affected by both the annealing temperature and rolling reduction. With higher degree of warm rolling, the ferrite grains are more refined and the carbide spheroidization is more significant, thus generating more austenite nucleation sites to enhance austenite formation, which results in higher martensite content in the 60 % warm-rolled samples at the same annealing temperature.
(3) Higher martensite fraction enhances both the YS and UTS of DP steels. In contrast, the UE was decreased with increasing martensite content. The 40 % warm-rolled sample annealed at 840 °C presents an impressive mechanical property with UTS of 1559 MPa and UE of 7.1 % among the laminate HMDP steels.

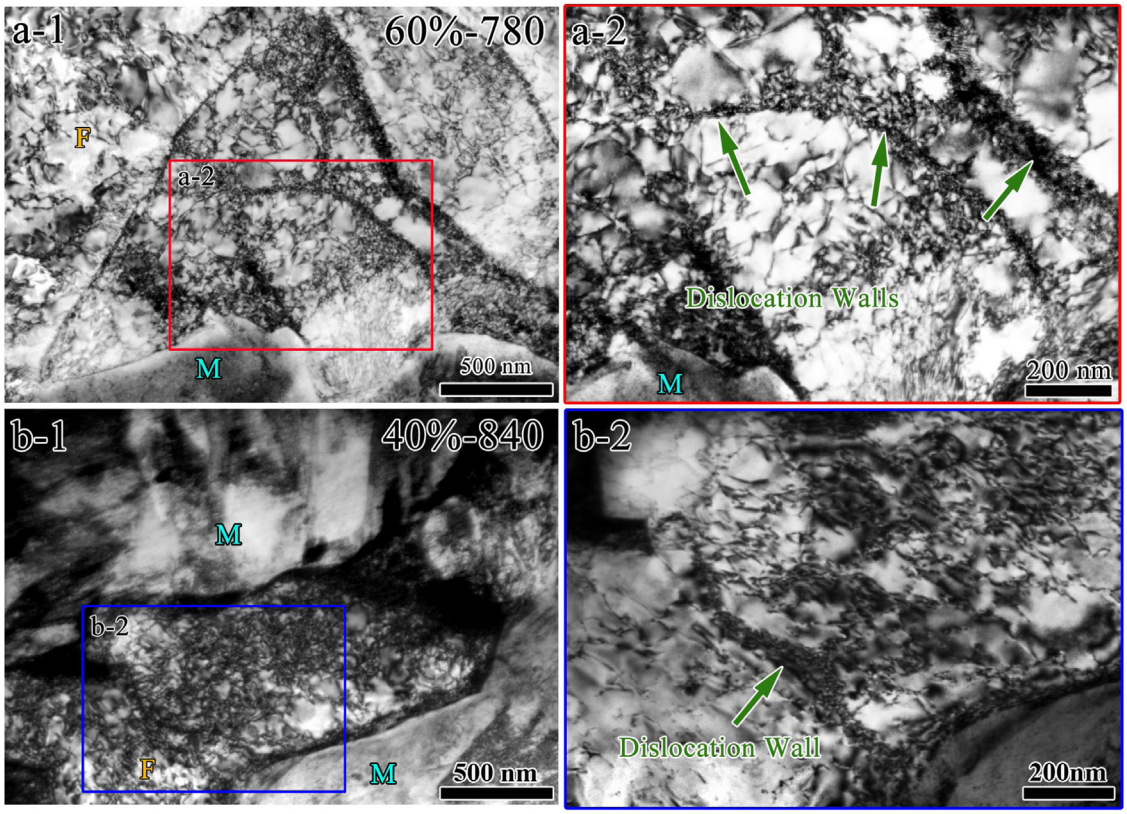

Fig. 9. TEM micrographs of 60 %-780 DP and 40 %-840 DP after tensile strain of 6%: (a-1) dislocations in ferrite of 60 %-780 DP; (a-2) enlarged image of the selected area in (a-1); (b-1) dislocations in ferrite of 40 %-840 DP; (b-2) enlarged image of the selected area in (b-1).

(4) The excellent strength-ductility synergy is contributed to its proposed laminate heterostructure feature, in which minor laminate ferrite grains are embedded in the hard martensite matrix. With higher martensite content, higher magnitude of Bauschinger effect and HDI stress were found in the laminate HMDP steels. It is mainly resulted from the development of meso-scale internal stresses distribution which is induced by the mechanical heterogeneity between ferrite and martensite. The enhanced strain hardening retarded the onset of necking in laminate HMDP steels.

Acknowledgments

This work was supported financially by the National Key R&D Program of China (No. 2017YFA0204403), the National Natural Science Foundation of China (Nos. 51931003, 51601094, 51601003, 51701097 and 51901103), the Fundamental Research Funds for the Central Universities (Nos. 30917011106 and 30918011342), the Natural Science Foundation of Jiangsu Province (Nos. BK20170843 and BK20180492). We also thank the technical support from the Jiangsu Key Laboratory of Advanced Micro&Nano Materials and Technology. The SEM and TEM experiments are performed at the Materials Characterization and Research Center of Nanjing University of Science and Technology.

References

[1] Q. Lai, L. Brassart, O. Bouaziz, M. Gouné, M. Verdier, G. Parry, A. Perlade, Y. Bréchet, T. Pardoen, Int. J. Plast. 80 (2016) 187–203.
[2] D. Gerbig, A. Srivastava, S. Osovski, L.G. Hector, A. Bower, Int. J. Fract. Mech. 209 (2018) 3–26.
[3] M.X. Huang, B.B. He, J. Mater. Sci. Technol. 34 (2018) 417–420.
[4] H. Mirzadeh, M. Alibeyki, M. Najafi, Metall. Mater. Trans. A 48 (2017) 4565–4573.
[5] F. Zhang, A. Ruimi, P.C. Wo, D.P. Field, Mater. Sci. Eng. A 659 (2016) 93–103.
[6] H. Ashrafi, M. Shamanian, R. Emadi, N. Saeidi, Mater. Sci. Eng. A 680 (2017) 197–202.
[7] Y. Cao, Y.B. Wang, X.H. An, X.Z. Liao, M. Kawasaki, S.P. Ringer, T.G. Langdon, Y.T. Zhu, Acta Mater. 63 (2014) 16–29.
[8] Y. Liu, M. Liu, X. Chen, Y. Cao, H.J. Roven, M. Murashkin, R.Z. Valiev, H. Zhou, Scr. Mater. 159 (2019) 137–141.
[9] W. Guo, Q.D. Wang, B. Ye, M.P. Liu, T. Peng, X.T. Liu, H. Zhou, Mater. Sci. Eng. A 540 (2012) 115–122.
[10] C. Haase, O. Kremer, W. Hu, T. Ingendahl, R. Lapovok, D.A. Molodov, Acta Mater. 107 (2016) 239–253.
[11] X.L. Ma, H. Zhou, J. Narayan, Y.T. Zhu, Scr. Mater. 109 (2015) 89–93.
[12] X. Wu, P. Jiang, L. Chen, F. Yuan, Y.T. Zhu, Proc. Natl. Acad. Sci. U.S.A. 111 (2014) 7197–7201.
[13] L.X. Sun, N.R. Tao, M. Kuntz, J.Q. Yu, K. Lu, J. Mater, Sci. Technol. 30 (2014) 731–735.
[14] X. Wu, M. Yang, F. Yuan, G. Wu, Y. Wei, X. Huang, Y. Zhu, Proc. Natl. Acad. Sci. U.S.A. 112 (2015) 14501–14505.
[15] X. Wu, Y. Zhu, Mater. Res. Lett. 5 (2017) 527–532.
[16] H. Zhou, C. Huang, X. Sha, L. Xiao, X. Ma, H.W. Höppel, M. Göken, X. Wu, K. Ameyama, X. Han, Y. Zhu, Mater. Res. Lett. 7 (2019) 376–382.
[17] Y. Zhu, X. Wu, Mater. Res. Lett. 7 (2019) 393–398.
[18] E. Fereiduni, S.S.G. Banadkouki, Mater. Des. 56 (2014) 232–240.
[19] W. Xue, J. Zhou, Y. Shen, W. Zhang, Z. Liu, J. Mater. Sci. Technol. 35 (2019) 1869–1876.
[20] W. Cao, M. Zhang, C. Huang, S. Xiao, H. Dong, Y. Weng, Sci. Rep. 7 (2017) 41459.
[21] H. Di, Q. Sun, X. Wang, J. Li, J. Mater. Sci. Technol. 33 (2017) 1561–1571.
[22] G.M. Xie, H.B. Cui, Z.A. Luo, W. Yu, J. Ma, G.D. Wang, J. Mater. Sci. Technol. 32 (2016) 326–332.
[23] H. Zhou, Q.D. Wang, B. Ye, W. Guo, Mater. Sci. Eng. A 576 (2013) 101–107.
[24] Y.I. Son, Y.K. Lee, K.-T. Park, C.S. Lee, D.H. Shin, Acta Mater. 53 (2005) 3125–3134.
[25] H. Azizi-Alizamini, M. Militzer, W.J. Poole, ISIJ Int. 51 (2011) 958–964.
[26] M. Yang, Y. Pan, F. Yuan, Y. Zhu, X. Wu, Mater. Res. Lett. 4 (2016) 145–151.
[27] Q. Lai, O. Bouaziz, M. Gouné, A. Perlade, Y. Bréchet, T. Pardoen, Mater. Sci. Eng. A 638 (2015) 78–89.
[28] M.C. Zhao, X.F. Huang, J.L. Li, T.Y. Zeng, Y.C. Zhao, A. Atrens, Mater. Sci. Eng. A 528 (2011) 8157–8168.
[29] L. Hao, M. Sun, N. Xiao, D. Li, J. Mater, Sci. Technol. 28 (2012) 1095–1101.
[30] L. Storojeva, D. Ponge, R. Kaspar, D. Raabe, Acta Mater. 52 (2004) 2209–2220.
[31] C.I. Garcia, A.J. De Ardo, Metall. Trans. A 12 (1981) 521–530.

[32] J. Huang, W.J. Poole, M. Militzer, Metall. Mater. Trans. A 35 (2004) 3363–3375.
[33] Y. Mazaheri, A. Kermanpur, A. Najafizadeh, A.G. Kalashami, Metall. Mater. Trans. A 47 (2016) 1040–1051.
[34] Q. Lai, M. Gouné, A. Perlade, T. Pardoen, P. Jacques, O. Bouaziz, Y. Bréchet, Metall. Mater. Trans. A 47 (2016) 3375–3386.
[35] H. Azizi-Alizamini, M. Militzer, W.J. Poole, Metall. Mater. Trans. A 42 (2010) 1544–1557.
[36] M. Kulakov, W.J. Poole, M. Militzer, Metall. Mater. Trans. A 44 (2013) 3564–3576.
[37] M. Calcagnotto, D. Ponge, D. Raabe, Mater. Sci. Eng. A 527 (2010) 7832–7840.
[38] L. Zhao, N. Park, Y. Tian, S. Chen, A. Shibata, N. Tsuji, Mater. Res. Lett. 5 (2017) 61–68.
[39] Z. Pan, B. Gao, Q. Lai, X. Chen, Y. Cao, M. Liu, H. Zhou, Materials 11 (2018) 1399.
[40] Y. Zhang, D. Zhan, X. Qi, Z. Jiang, J. Mater. Sci. Technol. 35 (2019) 1240–1249.
[41] B. Gao, X. Chen, Z. Pan, J. Li, Y. Ma, Y. Cao, M. Liu, Q. Lai, L. Xiao, H. Zhou, J. Mater. Sci. 54 (2019) 12898–12910.
[42] F. Lefevre-Schlick, O. Bouaziz, Y. Brechet, J.D. Embury, Mater. Sci. Eng. A 491 (2008) 80–87.
[43] S. Sodjit, V. Uthaisangsuk, Mater. Des. 41 (2012) 370–379.
[44] J. Zhou, A.M. Gokhale, A. Gurumurthy, S.P. Bhat, Mater. Sci. Eng. A 630 (2015) 107–115.
[45] N.H. Abid, R.K. Abu Al-Rub, A.N. Palazotto, Int. J. Solids Struct. 104-105 (2017) 8–24.
[46] Y. Liu, D. Fan, S.P. Bhat, A. Srivastava, Int. J. Plast. 125 (2020) 80–96.
[47] X. Zheng, H. Ghassemi-Armaki, A. Srivastava,Mater. Sci. Eng. A 774 (2020), 138924.
[48] J. Kadkhodapour, S. Schmauder, D. Raabe, S. Ziaei-Rad, U. Weber, M. Calcagnotto, Acta Mater. 59 (2011) 4387–4394.
[49] Q. Han, Y. Kang, P.D. Hodgson, N. Stanford, Scr. Mater. 69 (2013) 13–16.
[50] M.F. Ashby, Philos. Mag. Abingdon (Abingdon) 21 (1970) 399–424.
[51] N.A. Fleck, M.F. Ashby, J.W. Hutchinson, Scr. Mater. 48 (2003) 179–183.